ELSEVIER

Thermochimica Acta 303 (1997) 31–39

thermochimica acta

Influence of pH on the hydrothermal crystallization kinetics and crystal structure of ZrO_2

G. Štefanić[a,*], S. Popović[ab], S. Musić[a]

[a] *Ruđer Bošković Institute, P.O. Box 1016, 10001 Zagreb, Croatia*

[b] *Department of Physics, Faculty of Science, University of Zagreb, P.O. Box 162, 10001 Zagreb, Croatia*

Received 23 January 1997; received in revised form 13 May 1997; accepted 31 May 1997

Abstract

Differential scanning calorimetry was used to measure the heat evolved as zirconia samples are heated at constant rate. The data are used to deduce the kinetics of zirconia crystallization during hydrothermal treatments at pH 2, 7, 9.5 and 13. Hydrothermal crystallization was found to proceed much more slowly in the neutral pH medium than in the acidic or alkaline medium. The analogy between the rate of the hydrothermal crystallization of ZrO_2 and solubility of zirconium hydroxide was discussed. The results of phase analysis showed that metastable cubic zirconia, c-ZrO_2, could be produced by hydrothermal crystallization in the presence of NaOH as a stabilizing agent. The results of X-ray diffraction showed that, even at low pH, monoclinic zirconia, m-ZrO_2, was not the only product of the dissolution/precipitation mechanism of hydrothermal crystallization. It is concluded that in situ crystallization of amorphous zirconium hydroxide, if it occurs, is not a topotactic process. © 1997 Elsevier Science B.V.

Keywords: Crystallization kinetics; DSC; Raman; XRD; ZrO_2

1. Introduction

ZrO_2 can be crystallized by hydrothermal treatment or solid-state calcination of zirconium hydroxide. Generally, the hydrothermal treatment of zirconium hydroxide yields well-shaped and isolated, fine ZrO_2 particles, while solid-state calcination strongly affects the morphology and particle size due to the sintering effect. The hydrothermal method is, therefore, preferred in the production of fine zirconia powders for use in advanced ceramics. The processing variables (pH, concentration, temperature, time, etc.) have an important influence on hydrothermal crystallization. Hydrothermal treatment of highly acidic solutions or suspensions of zirconium hydroxide produced monoclinic zirconia, m-ZrO_2, [1–3], while solid-state calcination of zirconium hydroxide at ~500°C, precipitated at low pH, produced predominantly metastable tetragonal zirconia, t-ZrO_2, [4,5]. At high pH values the hydrothermal treatment of zirconium hydroxide yielded metastable t-ZrO_2 besides m-ZrO_2 and also metastable cubic zirconia, c-ZrO_2, in the presence of NaOH [6] or $CaCl_2$ [7] as a stabilizing agent. Adair et al. [8] showed that the solubility of zirconium hydroxide and m-ZrO_2 was nine orders of magnitude higher in high acidic and high alkaline media than in neutral or mild acidic media. Tani et al. [9] found that the addition of different mineralizers

*Corresponding author.

PII S0040-6031(97)00243-8

influenced the crystal structure of the ZrO_2 product. It was concluded that the formation of *m*-ZrO_2 by the hydrothermal treatment proceeded via a dissolution/precipitation mechanism [3,9], while the formation of *t*-ZrO_2 occurred as a result of structural rearrangement of amorphous zirconium hydroxide (topotactic crystallization) [9]. This conclusion was based on the results of neutron diffraction which showed that the amorphous ZrO_2 precursor possessed some structural features of *t*-ZrO_2 [10]. However, a recent structural examination [11,12] indicated that amorphous zirconium hydroxide possessed structural features more similar to *m*-ZrO_2 than to *t*-ZrO_2. On the basis of the DCS results and TG analysis, Štefanić et al. [13] concluded that the crystallization of *t*-ZrO_2 from amorphous zirconium hydroxide is a more complex phenomenon than a simple structural (topotactic) rearrangement. Denkewicz et al. [14] used the results of XRD to monitor the kinetics of hydrothermal crystallization of *m*-ZrO_2 and *t*-ZrO_2 at different pH.

In the present work, we used a different approach to the determination of the hydrothermal crystallization kinetics of ZrO_2 at different pH values. It is based on the measurement of changes in heat flow by differential scanning calorimetry (DSC). The obtained crystalline phases were monitored by X-ray powder diffraction (XRD) and in some cases by laser Raman spectroscopy.

2. Experimental

Aqueous suspensions of zirconium hydroxide at pH 2, 7, 9.5 and 13 were precipitated from the solution of $ZrO(NO_3)_2 \cdot 2H_2O$ salt with the addition of NaOH. The suspensions prepared were hydrothermally treated at 95°C for different times, then washed with doubly distilled water using a Sorvall RC2-B ultra-speed centrifuge (max. 20000 r.p.m.) and dried at 80°C for 24 h.

The phase composition of the samples was determined at RT using X-ray powder diffraction (Philips counter diffractometer, model MPD 1880) and in some cases by laser Raman (DILOR Z24) spectroscopy (Table 1). The volume fractions of *m*-ZrO_2 and

Table 1
Phase composition of the hydrothermally treated samples, as determined by X-ray diffraction and laser Raman spectroscopy

Sample	pH	Hydrotherm. treatment (h)	Phase composition		
			XRD (AVF)	XRD, *D* (nm)	laser Raman
Z2	2	0	Amorphous		
Z2a	2	8	„Zirconium nitrate"+$NaNO_3$		
Z2c	2	100	„Zirconium nitrate"+$NaNO_3$		
Z2d	2	300	*m*-ZrO_2 (VBDL)	3.5	
Z7	7	0	Amorphous		
Z7a	7	220	Amorphous		
Z7d	7	750	*m*-ZrO_2(0.75) +*t*-ZrO_2 and/or *c*-ZrO_2 (BDL)	13	
Z7e	7	1400	*m*-ZrO_2(0.77) +*t*-ZrO_2 and/or *c*-ZrO_2	27	m-ZrO_2+*t*-ZrO_2+ *c*-ZrO_2
Z9	9.5	0	Amorphous		Amorphous
Z9b	9.5	75	Amorphous		
Z9c	9.5	170			Amorphous + *c*-ZrO_2
Z9d	9.5	700	Amorphous		Amorphous + *c*-ZrO_2
Z13	13	0	Amorphous		
Z13b	13	3	Amorphous		
Z13c	13	7	*m*-ZrO_2(0.68) +*t*-ZrO_2 and/or *c*-ZrO_2 (VBDL)	6	m-ZrO_2+*c*-ZrO_2
Z13d	13	24	*m*-ZrO_2(0.70) +*t*-ZrO_2 and/or *c*-ZrO_2(VBDL)	7	*m*-ZrO_2+*c*-ZrO_2

Descriptions:
BDL – Broadened diffraction lines.
VBDL – Very broadened diffraction lines.
AVF – Approximate volume fraction.

Table 2
The results of DSC analysis of the samples (enthalpy, temperature and percentage of crystallization)

Sample	pH	Hydrotherm. treatment (h)	Crystallization		
			Enthalpy (kJ mol^{-1})	Peak maximum (°C)	%
Z2	2	0	−12	451	0
Z2a	2	8	−7	458	42
Z2b	2	60	0		100
Z2c	2	100	0		100
Z2d	2	300	0		100
Z7	7	0	−19	457	0
Z7a	7	220	−17	458	9
Z7b	7	300	−14	469	27
Z7c	7	500	−9	501	51
Z7d	7	750	−5	464	75
Z7e	7	1400	0		100
Z9	9.5	0	−21	461	0
Z9a	9.5	25	−16	485	25
Z9b	9.5	75	−8	529	63
Z9c	9.5	170	−1	572	95
Z9d	9.5	700	0		100
Z13	13	0	−19	475	0
Z13a	13	1	−13	526	32
Z13b	13	3	−6	540	65
Z13c	13	7	0		100
Z13d	13	24	0		100

t-ZrO_2 were determined by measuring integrated intensities of monoclinic $\bar{1}11$ and 111, as well as tetragonal 101 diffraction lines according to the procedure proposed by Toraya et al. [15]. For the samples which showed a pronounced broadening of diffraction lines, the crystallite size was estimated using the Scherrer equation $D = 0.9\lambda/(\beta\cos\theta)$, λ being the X-ray wavelength, θ the Bragg angle and β the pure full width at one half of the maximum intensity. The pure widths were obtained from the observed widths, after correction for instrumental broadening, for which the corresponding widths of the samples heated at 1300°C were used, following the procedure given in the literature [16]. The estimated D values are given in Table 1.

The samples prepared were heated inside a Model 7 Perkin–Elmer differential scanning calorimeter (DSC) up to 600°C with a scanning rate of 20°C per minute. During the heating nitrogen was used as a purging gas and circulating water as a coolant. The instrument was coupled to a personal computer loaded with a program for the processing of the obtained DSC curves. The molar values of the crystallization enthalpy, ΔH_c, were calculated using a procedure described in our previous papers [5,13]. The decrease of ΔH_c with increase of the time of hydrothermal treatments was used to monitor the kinetics of crystallization (Table 2). Thermogravimetric (TG) analysis of the Samples Z2, Z2b and $NaNO_3$ were carried out, up to 600°C, in a Mettler TG 50, with scanning rate of 20°C per minute. During the measurements argon was used as a purging gas.

3. Results and discussion

Fig. 1 shows the X-ray diffraction powder patterns of the samples precipitated at pH 13. After 3 h of the hydrothermal treatment no sign of a crystal phase could be observed (Sample Z13b), after 7 h (Sample Z13c) broad diffraction lines of m-ZrO_2 and metastable t-ZrO_2, or c-ZrO_2, phase appeared, and after 24 h (Sample Z13d) the diffraction line intensities increased, while the fractions of m-ZrO_2 and metastable t- or c-ZrO_2 remained unchanged, within the limits of experimental error. The laser Raman spectra of Samples Z13c and Z13d, hydrothermally treated for 7 and 24 h, respectively, showed one peak typical of

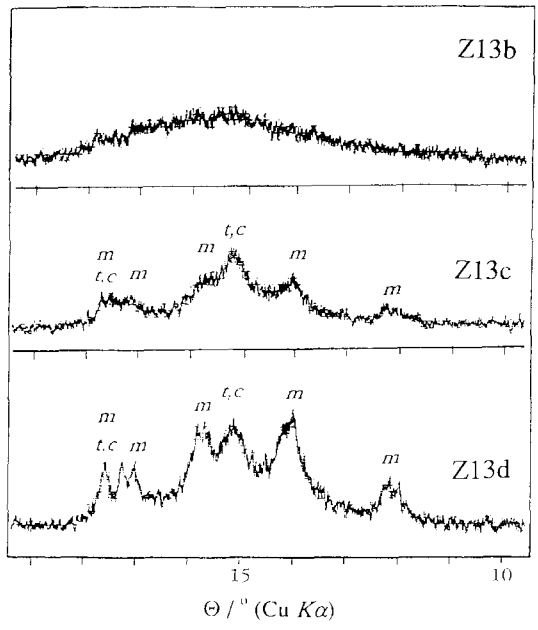

Fig. 1. Characteristic parts of X-ray diffraction powder patterns of Samples Z13b, Z13c and Z13d.

c-ZrO_2 [19] beside peaks typical of m-ZrO_2 [5,17,18]. The peaks, which may suggest the presence of t-ZrO_2 [5,17,18], were not observed, so it could be concluded that these two Samples (Z13c and Z13d) contain m-ZrO_2 and c-ZrO_2 phases.

The X-ray diffraction patterns of all the samples precipitated at pH 9.5 showed an amorphous material (Table 1). These results indicate a very short-range order of the reaction products obtained by the hydrothermal treatment at this pH. The laser Raman spectra of Samples Z9c and Z9d, hydrothermally treated for 170 and 700 h, respectively, showed a broad peak with a maximum at 600 cm^{-1} typical of c-ZrO_2. Similarly to this observation, Keramidas and White [17] observed the presence of tiny t-ZrO_2 crystallites in the laser Raman spectra of the sample which appeared to be amorphous for XRD. Appearance of the c-ZrO_2 phase, as a result of hydrothermal crystallization at pH ~10, was also reported by Cheng et al. [7].

Fig. 2 shows the X-ray diffraction powder patterns of the samples precipitated at pH 7. No sign of a crystal phase could be observed after 220 h of hydrothermal treatment (Sample Z7a); broad diffraction lines of m-ZrO_2 and metastable t-ZrO_2, or c-ZrO_2, appeared after 750 h (Sample Z7d); diffraction line

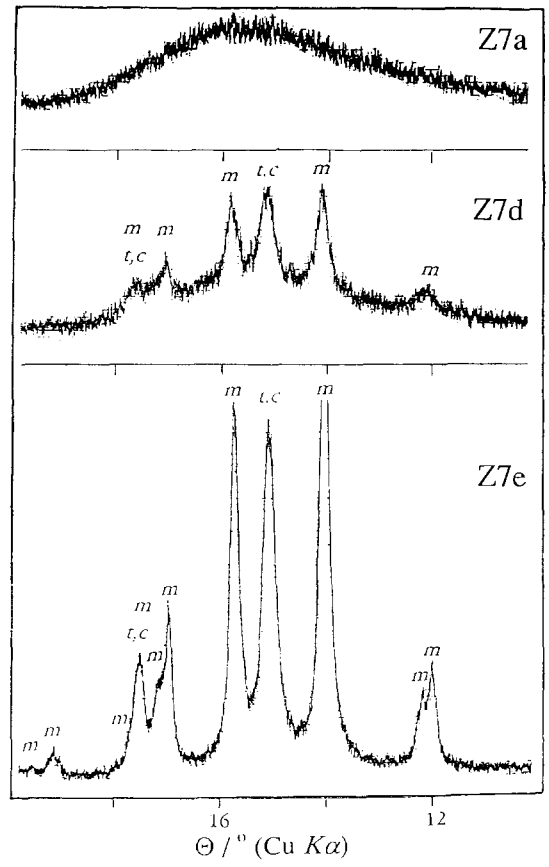

Fig. 2. Characteristic parts of X-ray diffraction powder patterns of Samples Z7a, Z7d and Z7e.

intensities increased after 1400 h, while the phase fractions remained approximately the same (Sample Z7e). These results indicated that the presence of m-ZrO_2 could not be attributed to the t-$ZrO_2 \rightarrow m$-ZrO_2 transition caused by hydrothermal treatment. The laser Raman spectrum of Sample Z7e, hydrothermally treated for 1400 h, showed peaks typical of m-ZrO_2 and t-ZrO_2. Presence of the very strong peak with maximum at 608 cm^{-1} (much stronger than peak at 640 cm^{-1}) indicates that c-ZrO_2 phase can also be present [19].

The results of X-ray diffraction of the samples precipitated at pH 2 showed, in agreement with the results of Morgan [2], that the first crystallized phase was a metastable form of zirconium nitrate, for which the observed powder data differed from any data mentioned in the literature. After a prolonged hydro-

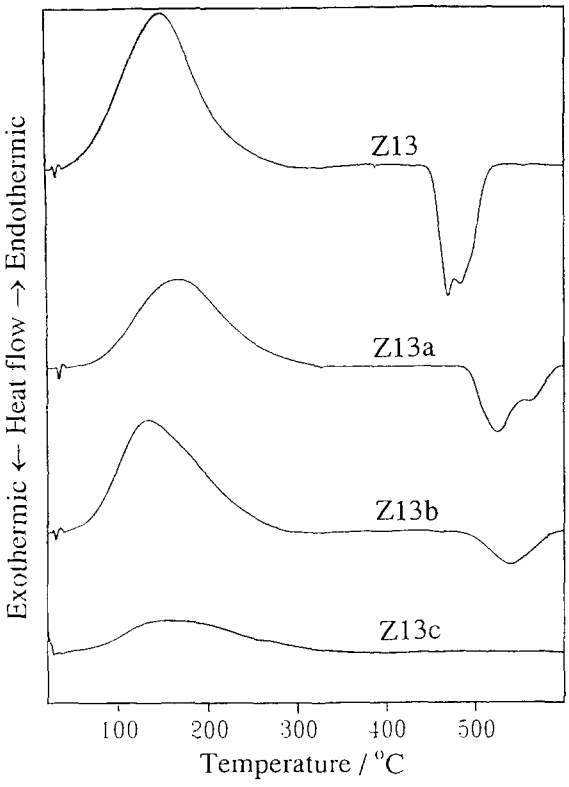

Fig. 3. DSC curves of the samples precipitated at pH 13 (Series Z13) and hydrothermally treated up to 24 h.

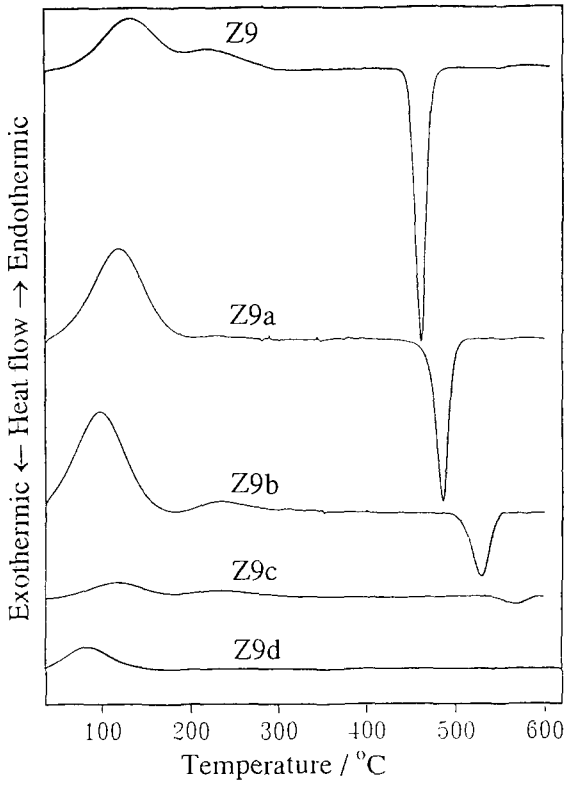

Fig. 4. DSC curves of the samples precipitated at pH 9.5 (Series Z9) and hydrothermally treated up to 700 h.

thermal treatment it transformed to *m*-ZrO_2 (Table 1). Similar results were reported by Kato et al. [21]. After hydrothermal treatment of a solution of zirconium salt containing SO_4^{2-} anions, they obtained metastable zirconium oxide sulfate that transformed to *m*-ZrO_2, following a prolonged hydrothermal treatment.

Fig. 3 shows the DSC curves of the samples precipitated at pH 13 and hydrothermally treated from zero to 7 h. The obtained curves contained one endothermic peak resulting from dehydration and one exothermic peak due to crystallization [22]. The exothermic peak gradually decreased with increasing hydrothermal treatment time and finally disappeared after 7 h, indicating that the process of crystallization had been completed. Similar results were observed for the samples precipitated at pH 9.5 (Fig. 4), but here the time needed for the exothermic peak of crystallization to disappear was much longer (~200 h). For the samples precipitated at pH 7 (Fig. 5) the exothermic peak of crystallization disappeared after 1400 h of hydrothermal treatment, indicating a further deceleration of the crystallization process. The DSC curves of the samples precipitated at pH 2 (Fig. 6) show another endothermic peak at ~300°C. Phase analysis shows that these samples contain large amount of nitrate group, partly bound to the zirconium and partly present in $NaNO_3$ (Table 1). DSC curve of $NaNO_3$ shows strong endothermic peak with maximum at 307°C resulting from the melting. TG curve of $NaNO_3$ shows very small change of the mass during the heating up to 600°C. On the other hand, TG analysis of the Samples Z2 and Z2b show continuous loss of mass in the temperature region of the first endothermic peak and, also, in the temperature region of the second endothermic peak. These results indicate that the second endothermic peak appear as a result of both melting of $NaNO_3$ and partial elimination of nitrate group present in these samples. The exothermic peak of crystallization of the samples precipitated at pH 2

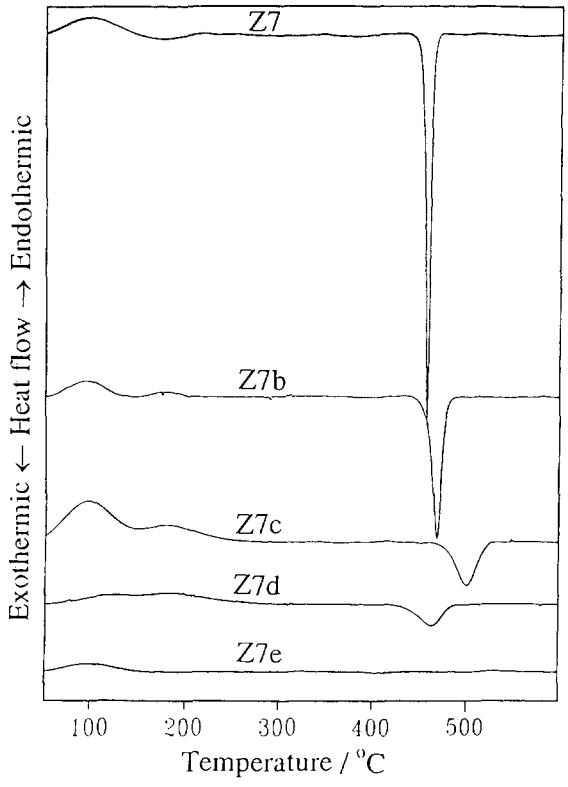

Fig. 5. DSC curves of the samples precipitated at pH 7 (Series Z7) and hydrothermally treated up to 1400 h.

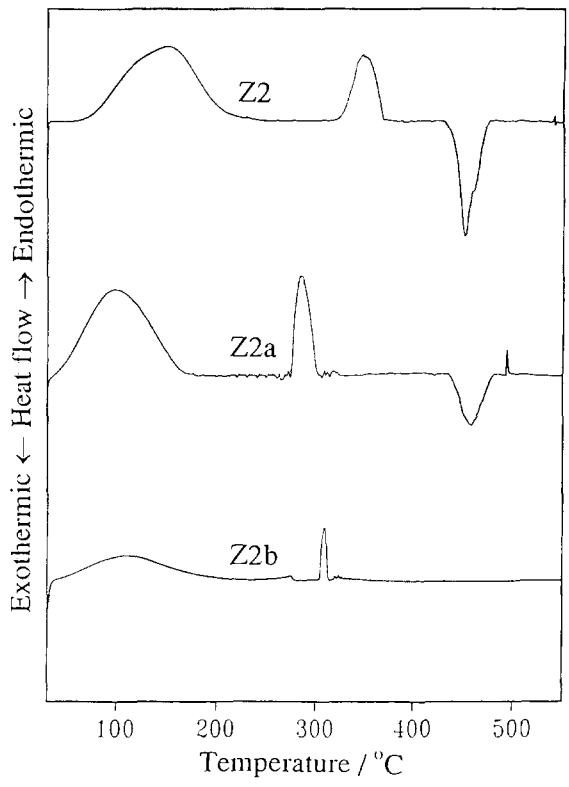

Fig. 6. DSC curves of the samples precipitated at pH 2 (Series Z2) and hydrothermally treated up to 300 h.

decreased more rapidly than the samples precipitated at pH 7 and 9.5.

The relation between the time of the hydrothermal treatment and the fraction of the crystal phase(s), as obtained from DSC curves, is shown in Fig. 7. These values were determined from the difference between ΔH_c of the starting amorphous Samples (Z2, Z7, Z9 and Z13) and ΔH_c of the hydrothermally treated samples, assuming zero for the starting samples and 100% for the samples with no exothermic peak of crystallization. All the curves indicated an increase of crystallization with increasing of the hydrothermal treatment time; however, the kinetics of this process depended on pH.

Fig. 8 shows the influence of pH on the time needed to crystallize 75% of the sample, i.e., the time after which the exothermic peak of crystallization decreased to 25% of its initial value. The left side of the curve is presented with a broken line because of the lack of information between pH 2 and 7. Regard-

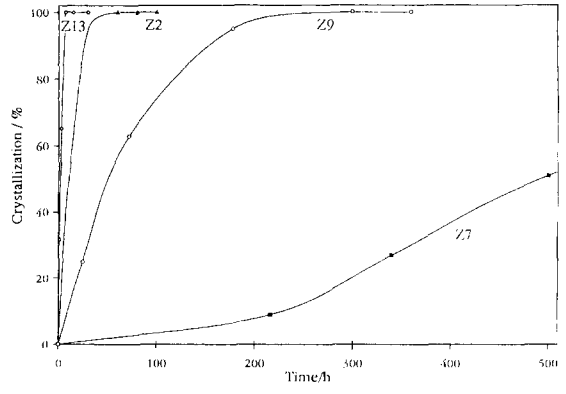

Fig. 7. The fraction of crystal phase(s) as a function of hydrothermal treatment times at different pH, as obtained from DSC curves.

less of this approximation, the results obtained clearly show that hydrothermal crystallization proceeds much more slowly in a neutral pH medium than in acidic or alkaline media.

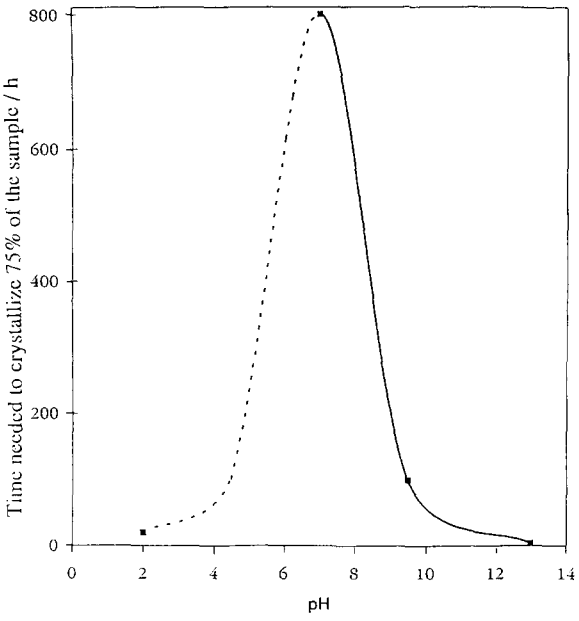

Fig. 8. The time needed to crystallize 75% of the sample as a function of pH.

The observed pH dependence of the crystallization rate can be explained by the influence of the solubility of zirconium hydroxide [8]. At high and low pH the crystallization rate is high, and so is solubility, while in a neutral medium both the crystallization rate and solubility are low indicating that, regardless of the pH, hydrothermal crystallization proceeds via a dissolution/precipitation mechanism.

Here, we would like to draw attention to the work of Denkewicz et al. [14]. These authors proposed, on the basis of their results, a model of m-ZrO_2 and t-ZrO_2 crystallization [9] and dependence of ZrO_2 solubility on pH and temperature [8]. According to this model, there are three control regimes for the crystallization of ZrO_2: At low pH the solubility is high, and the hydrothermal crystallization occurs via a dissolution/precipitation mechanism producing m-ZrO_2. In a neutral or mild acidic medium the solubility is very low, so that the crystallization occurs in situ by structural (topotactic) rearrangement of zirconium hydroxide. The product of hydrothermal crystallization in this region will be predominantly t-ZrO_2, and the presence of m-ZrO_2 can be attributed to the transition t-$ZrO_2 \rightarrow m$-ZrO_2 with prolonged hydrothermal treatment. At high pH the solubility of zirconium hydroxide is similar to the solubility at low pH (very high); yet, the obtained product is predominantly metastable t-ZrO_2. The authors concluded that in situ topotactic crystallization prevails at high pH, because of a higher energy state of the obtained zirconium hydroxide gel.

The interpretation of our results by the model of Denkewicz et al. [14] suggests: high crystallization rate in acidic medium resulting in formation of m-ZrO_2, low rate at intermediate pH where solubility is low, so that in situ crystallization of amorphous gel prevails with predominant formation of t-ZrO_2 and again high rate in alkaline medium, because of the high energy state of the zirconium hydroxide gel, resulting in predominant formation of t-ZrO_2.

Although, the model of Denkewicz et al. [14] can be accommodated within our crystallization kinetic observations, our phase analysis results differ from the results expected in this model. The model of Denkewicz et al. [14] is based on the conclusion that the dissolution/precipitation mechanism can produce only m-ZrO_2, while metastable t-ZrO_2 appears exclusively by in situ topotactic crystallization of zirconium hydroxide. On the other hand, if hydrothermal crystallization proceeds via the dissolution/precipitation mechanism in the whole pH range, it can be concluded that both m-ZrO_2 and t-ZrO_2 could be produced by this mechanism. Our X-ray powder diffraction results, as well as the results of Morgan [2] and Kato et al. [21], show that, even at low pH, m-ZrO_2 is not the exclusive product of the dissolution/precipitation mechanism of hydrothermal crystallization. Also, the results of phase analysis of zirconium hydroxide samples precipitated at pH 7 and 13 indicate that the presence of m-ZrO_2 cannot be attributed to the t-$ZrO_2 \rightarrow m$-ZrO_2 transition caused by hydrothermal treatment, as suggested by Denkewicz et al. [14].

Fig. 9 shows how the temperature of crystallization (position of the exothermic peak of crystallization in DSC curves) changes with the progress of the crystallization process. The temperature of crystallization of starting Sample Z13 is much higher than the temperatures of the other three starting Samples (Z2, Z7, Z9), contrary to the result which could be expected if the gel structure controlled regime at high pH [14] was adequate. Generally, the temperature of crystallization increases with an increase of the crystallization percentage (an exception was the change in the crystallization temperature between Samples Z7c and Z7d)

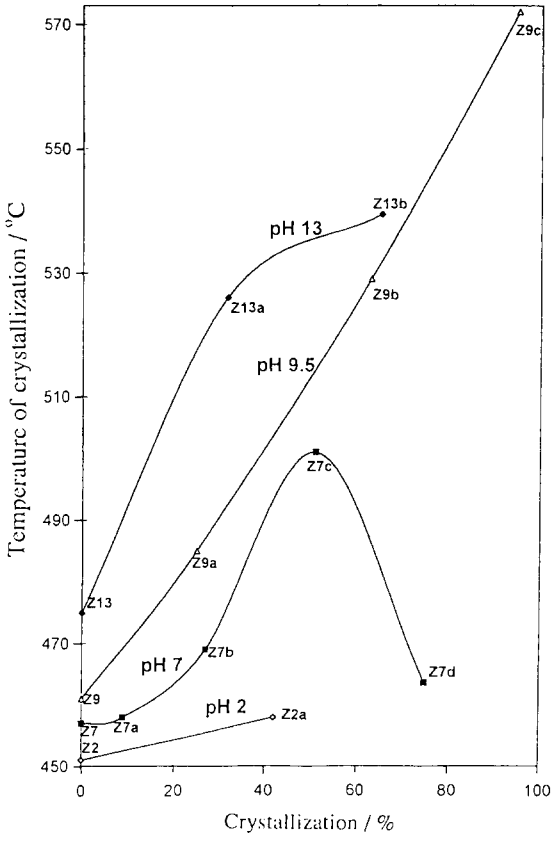

Fig. 9. The temperature of crystallization of zirconium hydroxide as a function of the fraction of crystal phase(s) (in %).

indicating that the presence of crystal phase hinders crystallization of the remaining amorphous phase. A similar effect was observed by Livage et al. [10]. These authors examined dependence of ZrO_2 crystallization percentage on the time of isothermal calcination. They found that the proportion of crystal phase in samples thermally treated below 350°C reached some limiting value, independent of the continued calcination time [10]. It is interesting to note the similarity between the changes in DSC curves (position and intensity of exothermic peak of the crystallization) caused by hydrothermal treatment and the changes caused by ball-milling of amorphous zirconium hydroxide [5,13].

4. Conclusion

The results of DSC analysis indicate that the rate of hydrothermal crystallization changes with the pH of the medium in a similar way as the solubility of zirconium hydroxide or ZrO_2 [8]. In acidic and alkaline medium the solubility and the rate of crystallization are high, and in neutral medium both the solubility and the rate of crystallization are low. No evidence of the existence of the gel structure controlled regime [14] could be found by phase analysis of the reaction products of the hydrothermal treatment. The X-ray diffraction powder patterns show that both m-ZrO_2 and a metastable t- or c-ZrO_2 phase appear as products of hydrothermal crystallization of zirconium hydroxide precipitated at pH 7 and 13. The phase fractions remain approximately the same after prolonged hydrothermal treatment, indicating that the presence of m-ZrO_2 cannot be attributed to the t-$ZrO_2 \rightarrow m$-ZrO_2 transition. Zirconium hydroxide precipitated at pH 2 crystallized firstly to some metastable form of zirconium nitrate that transformed with prolonged hydrothermal treatment to m-ZrO_2. It can be concluded that in situ crystallization of amorphous zirconium hydroxide, if it occurs, is not a topotactic process. The laser Raman spectra confirmed that the presence of NaOH could stabilize c-ZrO_2 phase [6,20].

References

[1] Sariçemen, H., Powder Technol., 27 (1980) 23.
[2] P.E. Morgan, J. Am. Ceram. Soc., 67 (1984) C–204.
[3] E. Tani, M. Yoshimura and S. Somiya, J. Am. Ceram. Soc., 64 (1981) C–181.
[4] B.H. Davis, J. Am. Ceram. Soc., 67 (1984) C–168.
[5] G. Štefanić, S. Musić and A. Sekulić, Thermochim. Acta., 273 (1996) 119.
[6] H. Nishizawa, N. Yamasaki and K. Matsuoka, J. Am. Ceram. Soc., 65 (1982) 343.
[7] H. Cheng, L. Wu, J. Ma, Z. Zhao and L. Qi, J. Mater. Sci. Lett., 15 (1996) 895.
[8] J.H. Adair, R.P. Denkewicz, F.J. Arrigada and K. Ossero-Asare, Ceram. Trans., Ceramic Powder Science, 1 (1988) 135.
[9] E. Tani, M. Yoshimura and S. Somiya, J. Am. Ceram. Soc., 66 (1983) 11.
[10] J. Livage, K. Doi and C. Mazieres, J. Am. Ceram. Soc., 51 (1968) 349.
[11] X. Turrillas, P. Barnes, D. Gascoigne, J.Z. Turner, S.L. Jones, C.J. Norman, C.F. Pygall and A.J. Dent, Radiat. Phys. Chem., 45 (1995) 491.
[12] Z. Yanwei, G. Fagherazzi and S. Polizzi, J. Mater Sci., 30 (1995) 2153.

[13] G. Štefanić, S. Musić and S. Popović, Thermochim. Acta, 259 (1995) 225.
[14] R.P. Denkewicz, K.S. TenHuisen and J.H. Adair, J. Mater. Res., 5 (1990) 2698.
[15] H. Toraya, M. Yoshimura and S. Somiya, J. Am. Ceram Soc., 67 (1984) C119.
[16] H.P. Klug and L.E. Alexander, X-ray Diffraction Procedures, 2nd edn., John Wiley and Sons, New York 1974, pp. 640–642, (Fig. 9.9).
[17] G. Keramidas and W.B. White, J. Am. Ceram. Soc., 57 (1974) 22.
[18] G. Štefanić, S. Musić, S. Popović and K. Furić, Croat. Chem. Acta, 69 (1996) 223.
[19] T. Hirata, E. Asari and M. Kitajima, J. Solid State. Chem., 110 (1994) 201.
[20] A. Benedetti, G. Fagherazzi and F. Pinna, J. Am. Ceram. Soc., 72 (1989) 467.
[21] E. Kato, M. Hirano and A. Nagi, J. Am. Ceram. Soc., 78 (1995) 2259.
[22] R.C. Mackenzie, Differential Thermal Analysis, Vol. 1, 2nd edn., Academic press INC., London 1973, pp. 296–297, (Fig. 9.10.).